

Electronic Supporting Information (ESI)

Modulation of the catalytic activity on Pt nanoparticles through charge-transfer interactions with metal–organic frameworks

Shotaro Yoshimaru,^a Masaaki Sadakiyo,^{*a,b} Aleksandar Staykov,^b Kenichi Kato,^c Miho Yamauchi^{*a,b}

^a Department of Chemistry, Faculty of Science, Kyushu University, Moto-oka 744, Nishi-ku, Fukuoka 819-0395, Japan. ^b International Institute for Carbon-Neutral Energy Research (WPI-I2CNER), Kyushu University, Moto-oka 744, Nishi-ku, Fukuoka 819-0395, Japan. ^c RIKEN SPring-8 Center, Kouto 1-1-1, Sayo-cho, Sayo-gun, Hyogo 679-5148, Japan.

E-mail: sadakiyo@i2cner.kyushu-u.ac.jp

Density functional theory calculation

Calculations in this study were performed with plane-wave density functional theory implemented in the Vienna ab initio simulation package.¹⁻⁴ The Perdew–Burke–Ernzerhof exchange-correlation functional was employed using projector-augmented wave pseudopotentials. We used the graphical visualization software package VESTA to analyze and visualize the optimized geometries.⁵ Spin-polarized calculations were performed with 400 eV cutoff energy. Geometry optimization was performed and all atomic coordinates and cell parameters were fully relaxed. The geometry optimization was performed with k-point sampling at the gamma points. Monkhorst–Pack k-point sampling was used to estimate the local potential of the investigated metal–organic frameworks (MOFs). The k-point mesh for Mg-MOF-74 was $2 \times 2 \times 8$, for Zn-MOF-74 $2 \times 2 \times 8$, for UiO-66-NH₂ $2 \times 2 \times 2$, and for HKUST-1 $2 \times 2 \times 2$. The ionization potentials of the MOFs were calculated as a difference between the vacuum level and the top level of valence band of the MOFs. The value of the vacuum level was taken at the center of the void or pore of each MOF structure. For Mg-MOF-74 and Zn-MOF-74, this point was selected with coordinates of 0.0, 0.0, 0.5 relative to the cell parameters. For HKUST-1 and UiO-66-NH₂, this point was selected with coordinates of 0.5, 0.5, 0.5 relative to the cell parameters. This approach has been reported in the literature.⁶

Preparation of support materials

Synthesis of UiO-66-NH₂ ($\{\text{Zr}_6\text{O}_4(\text{OH})_4(\text{bdc-NH}_2)_6\}_\infty$ ($\text{H}_2\text{bdc-NH}_2 = 2\text{-aminoterephthalic acid}$))

ZrCl₄ (11.52 g, 49.43 mmol) was dissolved in 2880 ml DMF. After sonication for 15 min, 2-aminoterephthalic acid (8.928 g, 49.29 mmol) was added to this solution, followed by further sonification for 15 min. The reaction mixture was heated for 24 h at 120 °C. The precipitate was separated by centrifugation and washed several times with DMF and MeOH. It was then dried overnight under vacuum at 160 °C. Elemental analysis (%) calcd for Zr₆O₄(OH)₄(C₆H₃C₂O₄NH₂)₆(H₂O)₇: C 30.66, H 2.57, N 4.47; found for C 30.52, H 2.56, N 4.51.

Synthesis of HKUST-1 ($\{\text{Cu}_3(\text{btc})_2\}_\infty$ ($\text{H}_3\text{btc} = 1,3,5\text{-benzenetricarboxylic acid}$))

Cu(NO₃)₂·3H₂O (20.8 g, 86.0 mmol) and 1,3,5-benzenetricarboxylic acid (10.0 g, 47.6 mmol) were dissolved in 500 ml mixed solvent (DMF:EtOH:distilled water = 1:1:1). After sonication for 15 min, the solution was heated for 20 h at 85 °C. The precipitate was separated by decantation and washed with DMF. The collected product was immersed in chloroform (4 days, replenished 3 times). After filtration, the precipitate was washed with distilled water and MeOH. It was then dried overnight under vacuum at 160 °C. The product was refluxed in MeOH for a day and again dried overnight under vacuum at 160 °C. The resulting product was stirred in DMF for 26 h at 70 °C, separated by centrifugation, washed

with MeOH, and evacuated to dryness overnight, under vacuum, at 160 °C. Elemental analysis (%) calcd for $\text{Cu}_3\text{C}_{18}\text{H}_6\text{O}_{12}$: C 35.74, H 1.00; found for C 35.63, H 1.00.

Synthesis of Zn-MOF-74 ($\{\text{Zn}_2(\text{dobdc})\}_\infty$ ($\text{H}_4\text{dobdc} = 2,5\text{-dihydroxyterephthalic acid}$))

$\text{Zn}(\text{NO}_3)_2 \cdot 6\text{H}_2\text{O}$ (22.6 g, 76.0 mmol) and 2,5-dihydroxyterephthalic acid (5.00 g, 26.0 mmol) were dissolved in 1000 ml DMF. After sonication for 10 min, distilled water (50 ml) was added to the solution, followed by heating at 100 °C for 20 h. The precipitate was separated by decantation, washed with DMF, and immersed in MeOH (5 days, replenished 2 times). After filtration, this precipitate was washed with distilled water and MeOH, refluxed in MeOH for 30 h, and separated by centrifugation. The sample was dried at 160 °C under vacuum for 10 h. Elemental analysis (%) calcd for $\text{Zn}_2(\text{C}_8\text{H}_2\text{O}_6)(\text{H}_2\text{O})_{7.2}$: C 21.14, H 3.64; found for C 21.03, H 3.61.

Synthesis of Mg-MOF-74 ($\{\text{Mg}_2(\text{dobdc})\}_\infty$)

$\text{Mg}(\text{NO}_3)_2 \cdot 6\text{H}_2\text{O}$ (31.4 g, 122 mmol) and 2,5-dihydroxyterephthalic acid (7.39 g, 37.3 mmol) were dissolved in a mixed solvent of 2970 ml DMF, 198 ml EtOH, and 198 ml distilled water. After sonication for 15 min, this solution was heated for 21 h at 125 °C. The precipitate was separated by decantation and immersed in MeOH (2 days, replenished 5 times). It was then filtered and dried for 6 h under vacuum at 250 °C. Elemental analysis (%) calcd for $\text{Mg}_2(\text{C}_8\text{H}_2\text{O}_6)(\text{H}_2\text{O})_{2.2}$: C 34.03, H 2.28; found for C 33.79, H 1.93.

Preparation of Pt/MOFs

As in our previous experiments,⁷ MOF (Zn-MOF-74, Mg-MOF-74, HKUST-1, UiO-66-NH₂)-supported Pt catalysts (**Pt/MOF**) were prepared by irradiating plasma shots of an arc plasma gun (ULVAC ADP-3P-N2) with a Pt source in a vacuum chamber. During the arc plasma deposition (APD) experiments, the MOF supports were continuously stirred in a pot which was kept at 18 °C using a water-cooling device. The number of plasma shots for each MOF was summarized in the Table S1.

Table S1. Support amounts and the numbers of plasma shots for the APD experiments.

	Pt/Zn-MOF-74	Pt/Mg-MOF-74	Pt/HKUST-1	Pt/UiO-66-NH ₂
Support (g)	7.32	7.28	4.45	6.05
Shot	6600	8200	5200	8600

Measurements

X-ray powder diffraction (XRPD) measurements were conducted using a synchrotron X-ray source on the RIKEN Materials Science Beamline (BL44B2)⁸ at SPring-8 ($\lambda = 1.080 \text{ \AA}$) or Rigaku SmartLab diffractometer (Cu- $K\alpha$). Scanning transmission electron microscopy (STEM) observations and STEM coupled with energy dispersive X-ray spectrometry (STEM-EDS) were performed using a JEOL JEM-ARM 200F operated at 200 kV accelerating voltage. Inductively coupled plasma-atomic emission spectroscopy (ICP-AES) was conducted with a Thermo-Fisher iCAP6300. Pulse chemisorption measurements for H₂ were performed using BELCAT-A (BEL Japan, Inc.). N₂ adsorption isotherms were measured to estimate BET surface area using BELsorp-max (BEL Japan, Inc.) at 77 K. X-ray photoelectron spectroscopy (XPS) was performed using an ULVAC-PHI PHI 5000 VersaProbe II (Al- $K\alpha$). Binding energies obtained by XPS were calibrated with C1s spectra of carbon tape on the sample holder at 284.6 eV. Note that unidentified broad peaks around 75–78 eV were necessary to be used for the fitting of HKUST-1 data, which is probably attributable to Cu3p peaks.⁹ Ultraviolet photoelectron spectroscopy (UPS) was also performed using the ULVAC-PHI PHI 5000 VersaProbe II (He I, $h\nu = 21.2 \text{ eV}$) with a bias (–6.0 or –11.0 V) applied to the sample holder. Gold wire (25 μm) was used to avoid charge-up on the surfaces of the samples. Ionization potentials (E_I) obtained by the UPS were estimated by the following equation.

$$E_I = 21.2 - (E_{\text{cutoff}} - E_{\text{HOMO}})$$

CO oxidation reaction condition A (for T_{50})

The CO oxidation reaction with the condition A was performed with ~12 mg of catalysts, containing the same Pt amount, using BELCAT-A (BEL Japan, Inc.). The gas products were constantly monitored using BEL-MASS quadrupole mass spectrometer (BEL Japan, Inc.), while heating to 300 °C at a rate of 1.5 °C min⁻¹. A reaction gas mixture of 1% CO, 28% O₂, and 71% He was passed over the catalysts at room temperature before the reaction. Total flow rate and gas hourly space velocity (GHSV) were 50 ml min⁻¹ and 250000 ml g⁻¹ h⁻¹, respectively. The CO conversion was calculated according to the following equation:

$$\text{CO conversion (\%)} = (([\text{CO}]_{\text{inlet}} - [\text{CO}]_{\text{out}}) / [\text{CO}]_{\text{inlet}}) \times 100$$

where $[\text{CO}]_{\text{inlet}}$ and $[\text{CO}]_{\text{out}}$ represent the inlet and outlet concentrations of CO, respectively.

CO oxidation reaction condition B (for turnover frequency)

The CO oxidation reaction with the condition B was performed with 50 mg of catalysts, containing the same Pt amount using tubular quartz reactor in tubular furnace. The gas products were analyzed using thermal conductivity detector (TCD) gas chromatography (Shimadzu, GC-8A) equipping an

active carbon column (GL science, mesh 60/80, ID 3 mm ϕ , 2 m). A reaction gas mixture of 2% CO, 18% O₂, and 80% He was passed over the catalysts at room temperature before the reaction. Total flow rate and gas hourly space velocity (GHSV) were 50 ml min⁻¹ and 60000 ml g⁻¹ h⁻¹, respectively. The CO conversion was calculated according to the same equation with the condition A.

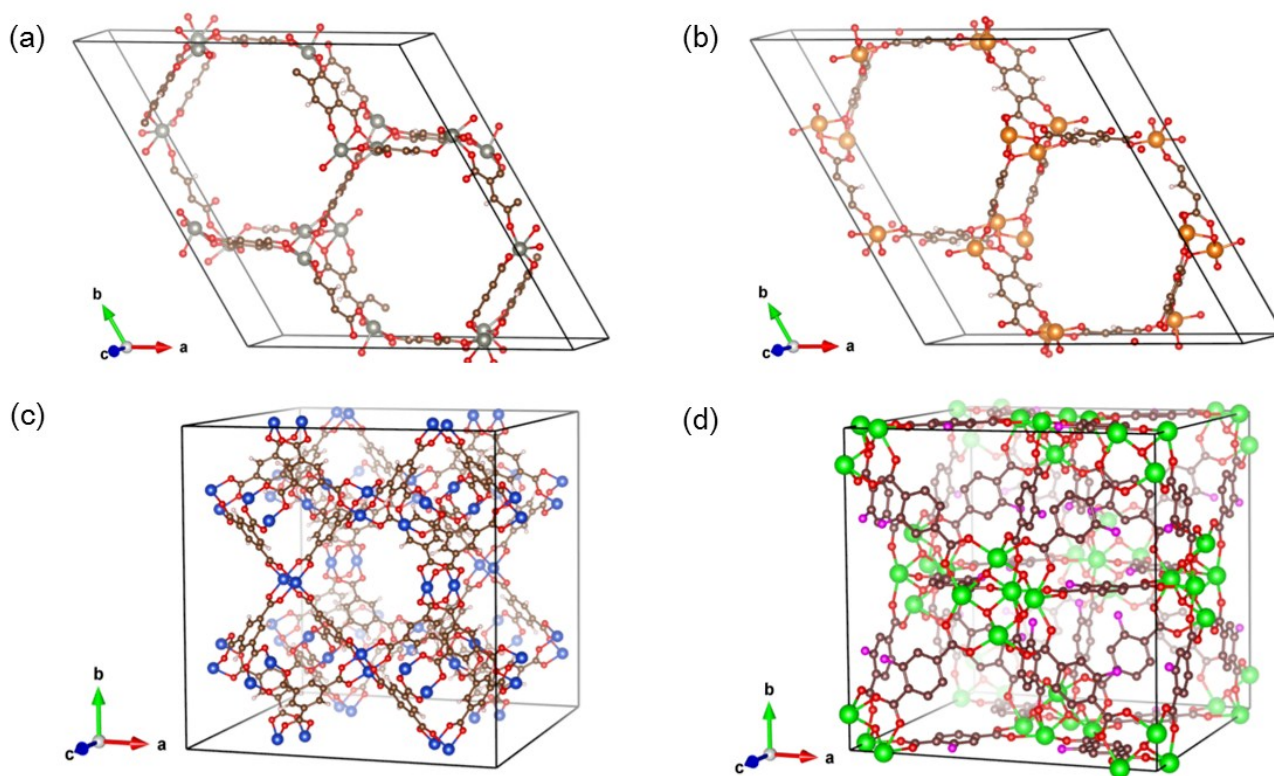


Fig. S1 Optimized geometries of (a) Zn-MOF-74, (b) Mg-MOF-74, (c) HKUST-1 and (d) UiO-66-NH₂, used for the DFT calculation. Zn, Mg, Cu, Zr, C, N, and O are represented by gray, orange, blue, green, brown, purple, and red, respectively.

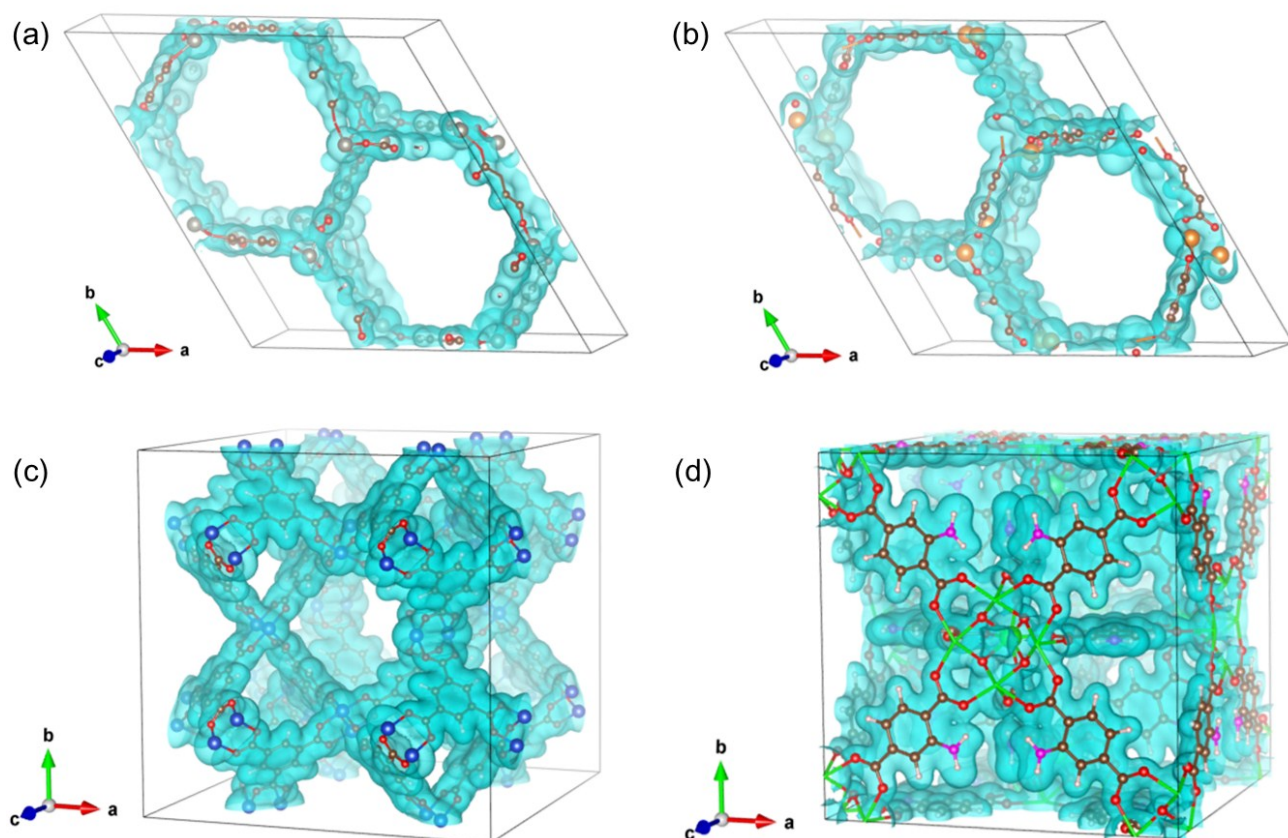


Fig. S2 Iso-electron density surfaces obtained from the DFT calculations of MOFs, (a) Zn-MOF-74, (b) Mg-MOF-74, (c) HKUST-1, and (d) UiO-66-NH₂.

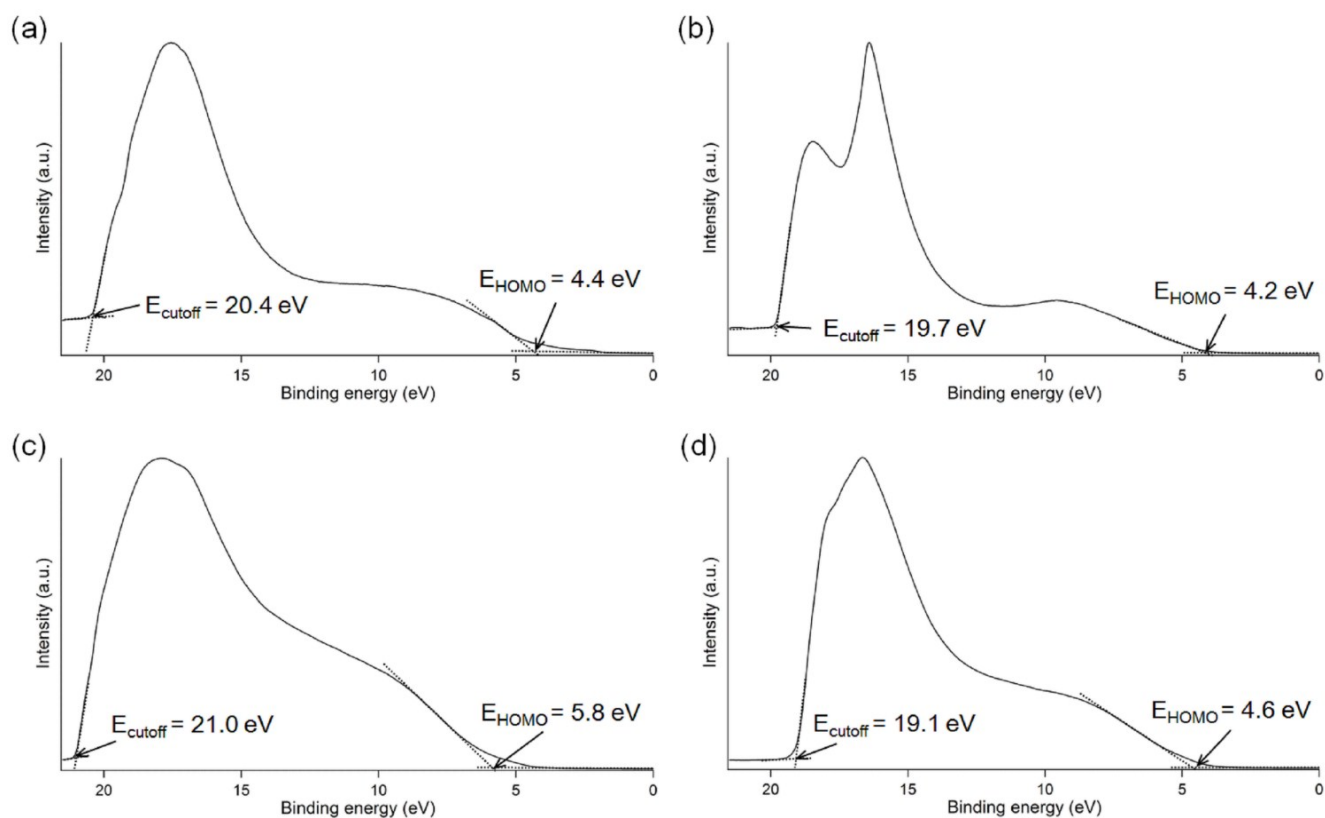


Fig. S3 UPS spectra of (a) Zn-MOF-74, (b) Mg-MOF-74, (c) HKUST-1, and (d) UiO-66-NH₂.

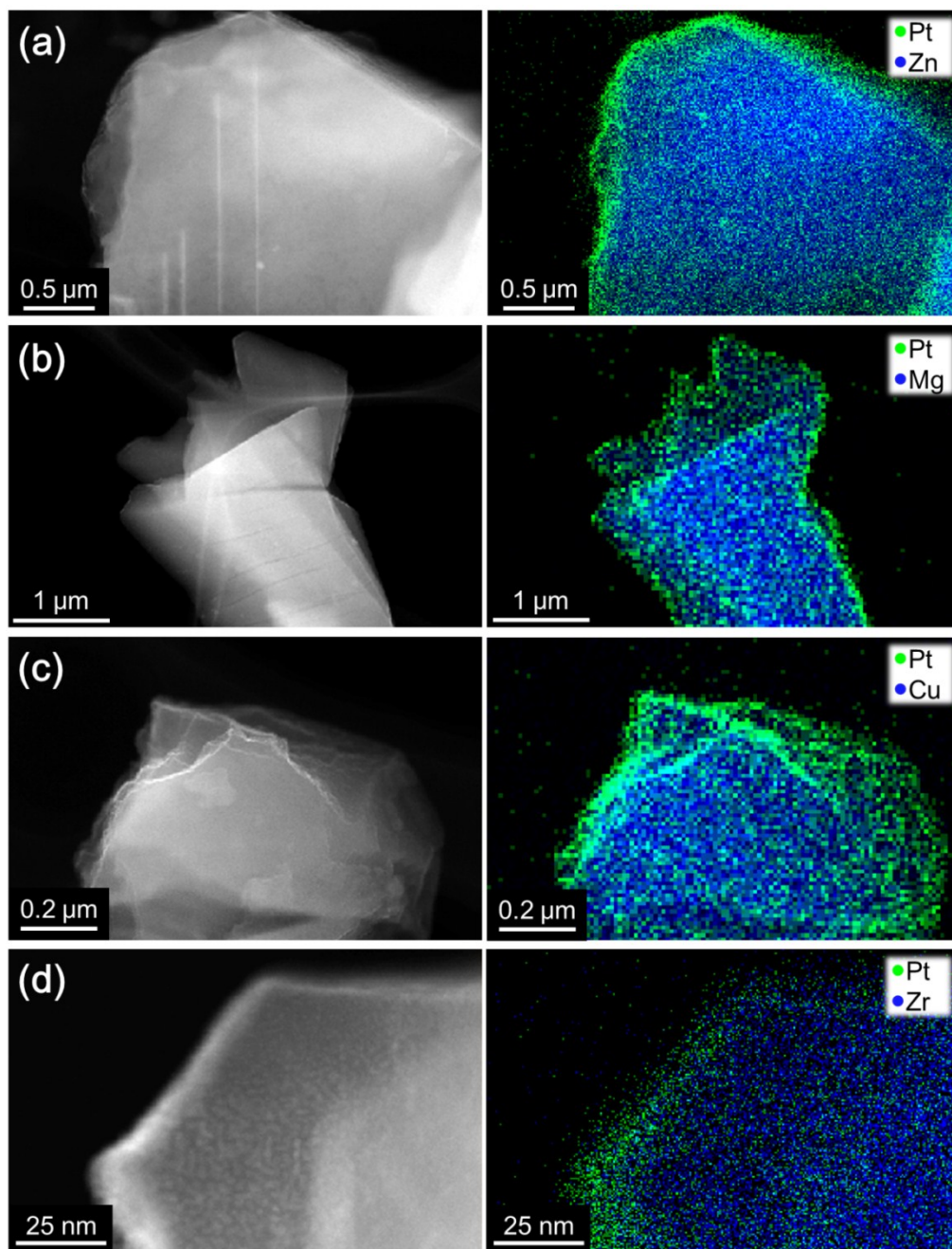


Fig. S4 (left) High-angle annular dark-field (HAADF)–STEM images and (right) STEM–EDS maps of (a) Pt/Zn-MOF-74, (b) Pt/Mg-MOF-74, (c) Pt/HKUST-1, and (d) Pt/UiO-66-NH₂. Green and blue correspond to EDS signals from deposited metal elements (Pt-M) and central metals of MOFs (Zn-L, Mg-K, Cu-K or Zr-K), respectively.

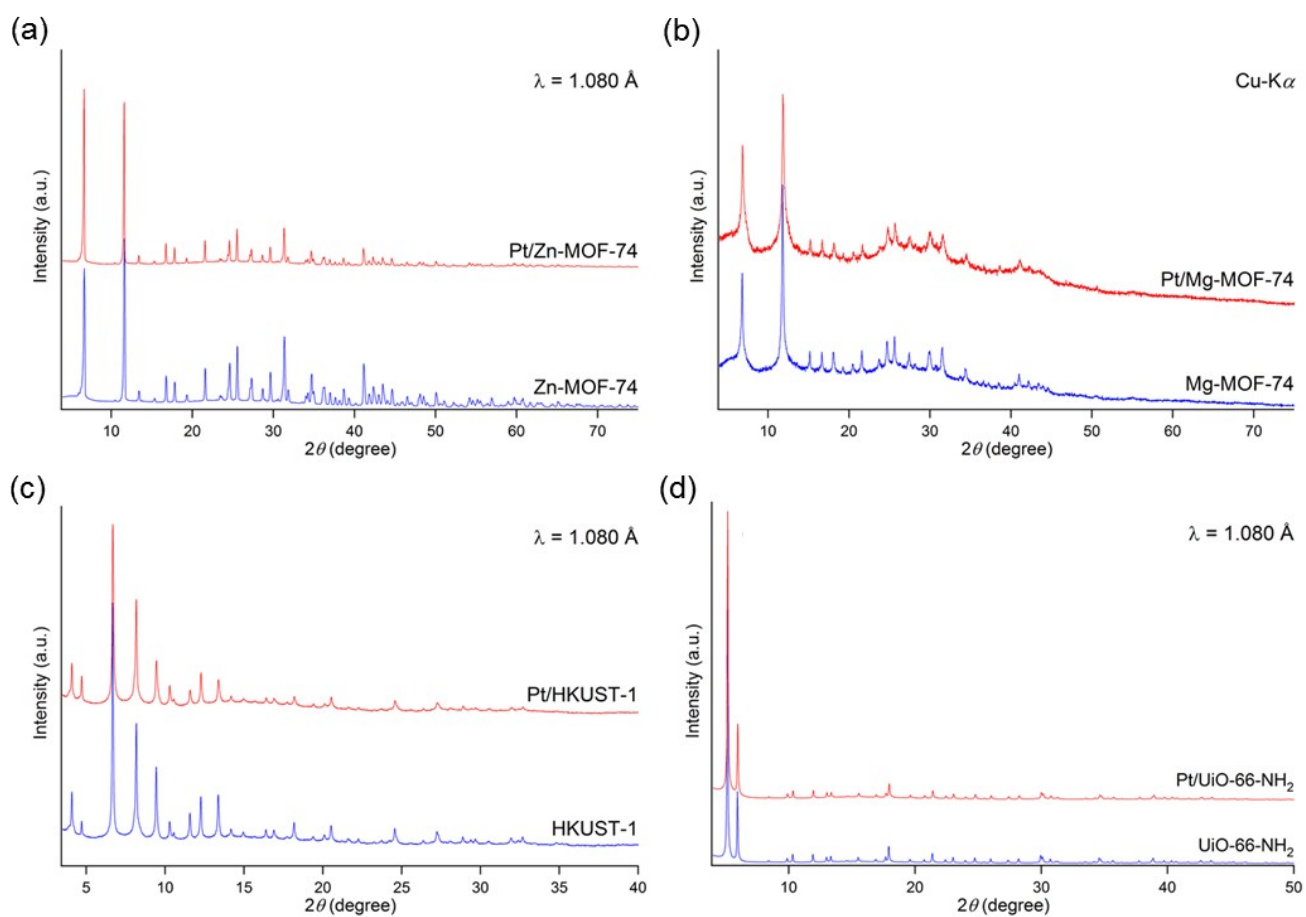


Fig. S5 XRPD patterns of (a) Zn-MOF-74, (b) Mg-MOF-74, (c) HKUST-1, and (d) UiO-66-NH₂ before and after the APD experiments.

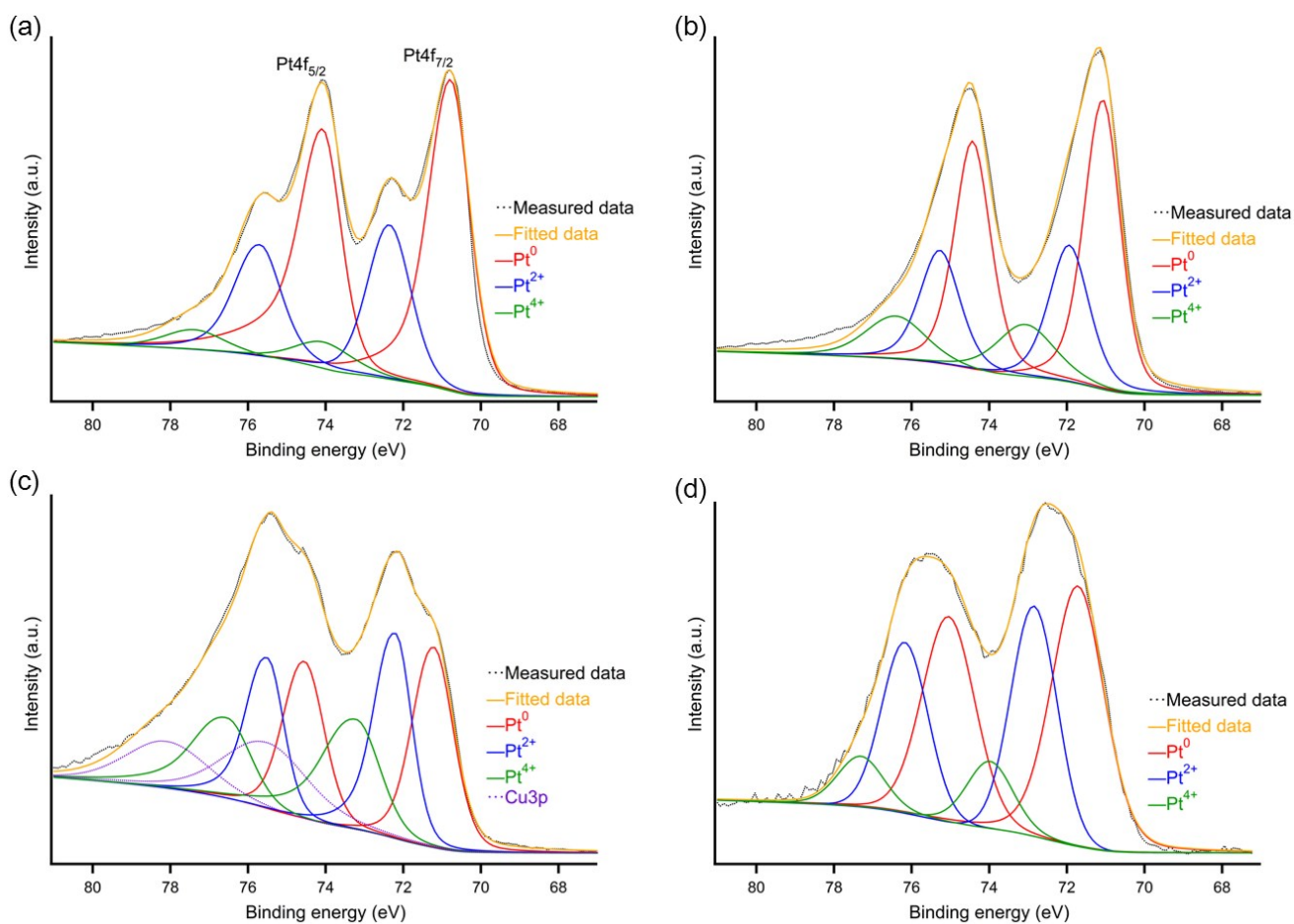


Fig. S6 XPS spectra of Pt4f of (a) **Pt/Zn-MOF-74**, (b) **Pt/Mg-MOF-74**, (c) **Pt/HKUST-1** and (d) **Pt/UiO-66-NH₂**.

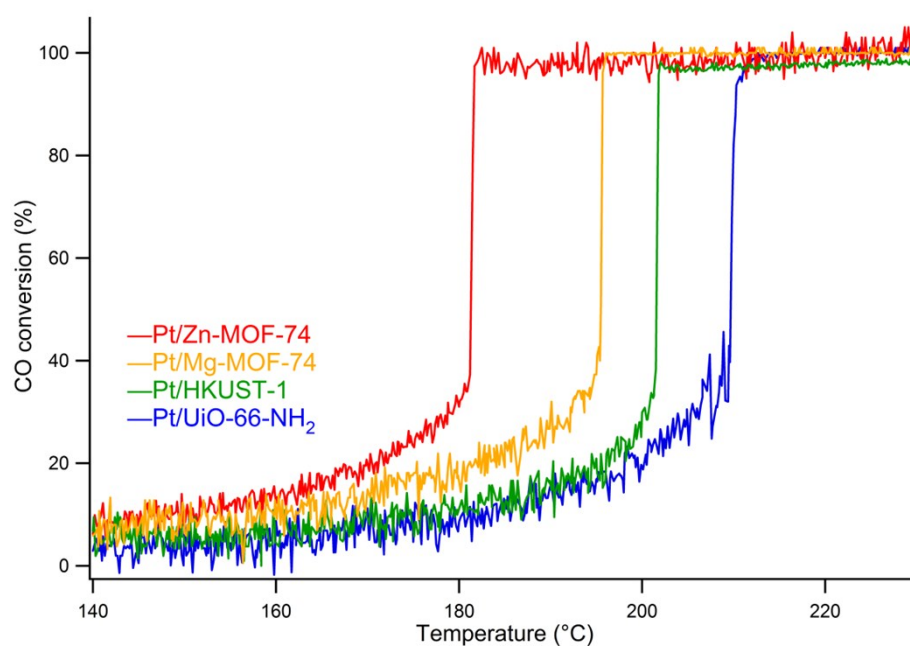


Fig. S7 Temperature dependence of CO conversion of **Pt/MOFs**.

Table S2. The amount of adsorbed H₂ on the loaded Pt NPs, measured by pulse chemisorption.

	Pt/Zn-MOF-74	Pt/Mg-MOF-74	Pt/HKUST-1	Pt/UiO-66-NH ₂
Adsorbed H ₂ (μmol g ⁻¹)	5.6	6.2	4.4	2.4

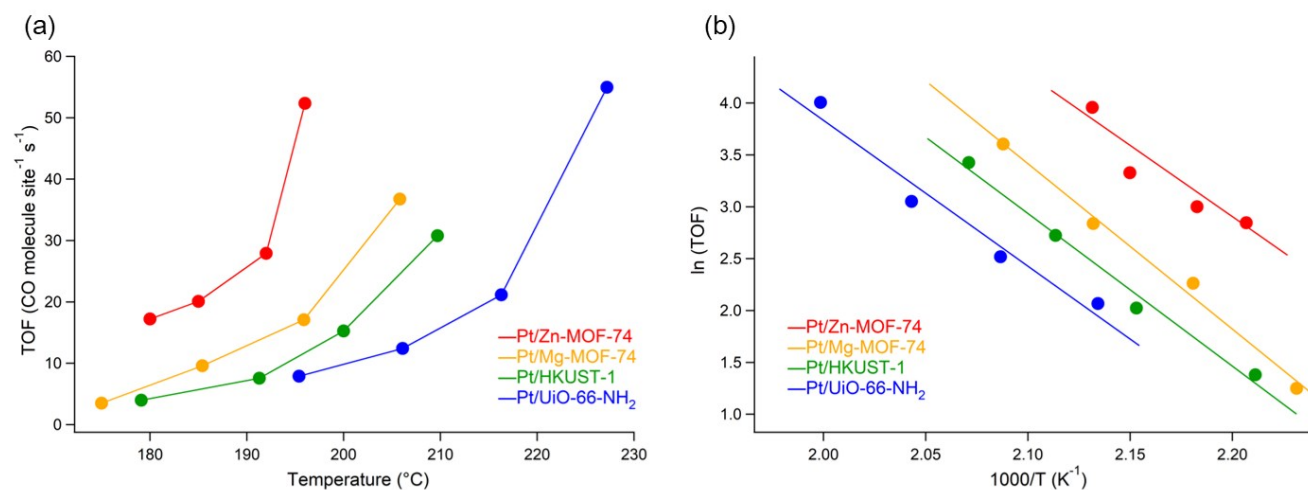


Fig. S8 (a) TOFs of Pt/MOFs for CO oxidation reaction at each temperature (condition B) and (b) Arrhenius plots of the TOFs.

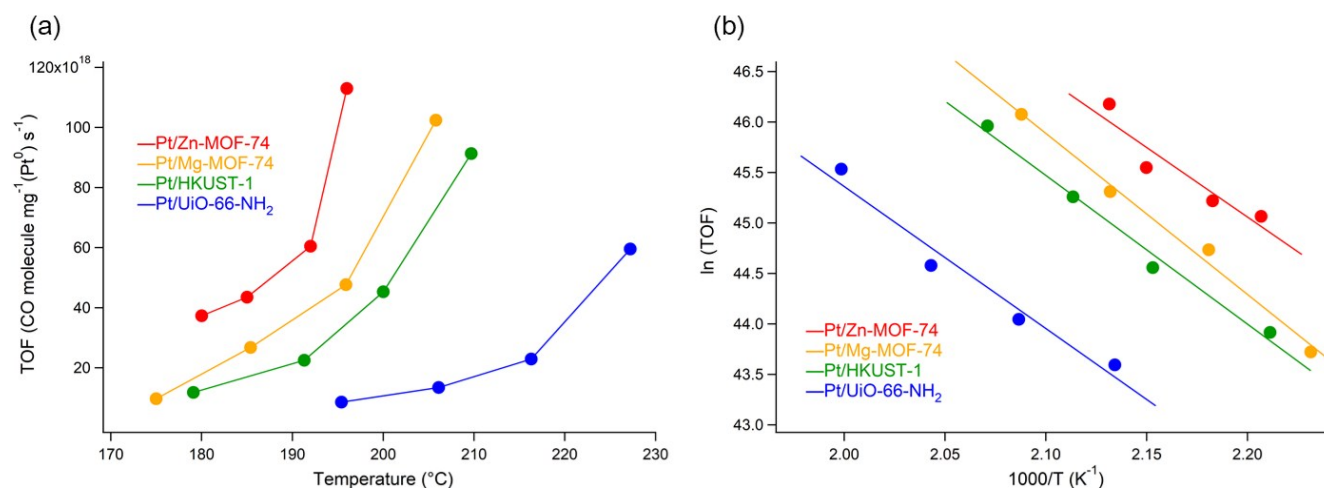


Fig. S9 (a) TOFs of Pt/MOFs, normalized by the weight of Pt⁰ included in the catalysts (estimated from the peak area ratio of the XPS spectra), for CO oxidation reaction and (b) Arrhenius plots of the TOFs.

REFERENCES

1. G. Kresse, J. Hafner, *Phys. Rev. B* **1993**, *47*, 558.
2. G. Kresse, J. Furthmüller, *Phys. Rev. B* **1996**, *54*, 11169.
3. G. Kresse, J. Furthmüller, *Comput. Mater. Sci.* **1996**, *6*, 15-50.

4. P. E. Blöchl, *Phys. Rev. B* **1994**, *50*, 17953.
5. K. Momma, F. Izumi, *J. Appl. Crystallogr.* **2011**, *44*, 1272–1276.
6. K. T. Butler, C. H. Hendon, A. Walsh, *J. Am. Chem. Soc.* **2014**, *136*, 2703–2706.
7. M. Sadakiyo, S. Yoshimaru, H. Kasai, K. Kato, M. Takata, M. Yamauchi, *Chem. Commun.*, **2016**, *52*, 8385–8388.
8. K. Kato, H. Tanaka, *Advances in Physics: X* **2016**, *1*, 55–80.
9. M. T. Anthony, M. P. Seah, *Surf. Inter. Anal.* **1984**, *6*, 107–115.